Physics-based Approach to Density Estimation and Prediction using Orbital Debris Tracking Data

Shaylah Mutschler
University of Colorado Boulder
Penina Axelrad, Tomoko Matsuo, Eric Sutton
University of Colorado Boulder

ABSTRACT

A key requirement for accurate trajectory prediction and Space Situational Awareness (SSA) is knowledge of the non-conservative forces affecting space objects. These effects vary temporally and spatially and are primarily driven by the dynamical behavior of space weather. Existing SSA algorithms adjust space environment models based on observations of calibration satellites. However, lack of sufficient data and mismodeling of non-conservative forces can cause inaccuracies in space object motion prediction, especially for uncontrolled debris objects. On the other hand, the uncontrolled nature of debris objects can make them particularly sensitive to the variations in space weather. Our research takes advantage of this behavior by utilizing observations of debris objects to infer the space environment parameters controlling their motion.

We explore rigorous and practically realizable means to utilize debris objects as passive, indirect sensors of the space environment. The focus is on atmospheric density for more accurate prediction of low Earth orbit object motion. In our previous work, a Partially Orthogonal Ensemble Kalman Filter (POEnKF) was implemented to assimilate observations of multiple debris objects and estimate atmospheric density in addition to the position and velocity of each debris object. In this work, a methodology is developed that aims to estimate forcing parameters of a physics-based space environment model to allow for improved density estimates and predictions. This tool consists of two filters: an Unscented Kalman Filter (UKF) and Particle Filter (PF). The UKF estimates acceleration due to drag and is able to follow its cyclic nature after about one orbital period, 90 minutes, of measurements. This information is passed to the PF to estimate forcing parameters of a physics-based space environment model, the Thermosphere-Ionosphere-Electrodynamics General Circulation Model (TIE-GCM). The overall tool performance is evaluated by comparing the true and estimated density; the latter is generated via TIE-GCM using the estimated forcing parameters as input.

1. INTRODUCTION

Our research utilizes debris objects to sense their local space environment. We focus on the low Earth orbital regime where mismodeling of atmospheric drag is the largest contributor to orbit prediction error. Current methods that estimate or model atmospheric density can be categorized as either empirical or physics-based approaches. Empirical models are computationally fast, but only represent the climatological atmospheric conditions. Physics-based models incorporate current knowledge of atmospheric conditions to provide forecasts, but require substantially more computing power than empirical models. Here, a methodology is described that aims to estimate forcing parameters of a physics-based space environment model to allow for improved density estimates and predictions. By improving space object predictions we hope to decrease the number of unnecessary satellite maneuvers executed to avoid debris objects. Thereby, increasing satellite mission lifetime and improving overall space situational awareness to the benefit of all space operations.

1.1 Atmospheric Density

An object in Low Earth Orbit (LEO) experiences atmospheric drag caused by particles in the atmosphere colliding with the surface of the object. Drag acts primarily in the opposite direction of the velocity vector to decrease the speed of an object. The magnitude of the force due to drag is directly dependent on neutral density (number of particles in the atmosphere). This is generally modelled in the equation of acceleration due to drag,

Copyright © 2019 Advanced Maui Optical and Space Surveillance Technologies Conference (AMOS) – www.amostech.com

$$a_{drag} = -\frac{1}{2}\rho\frac{C_D A}{m}v_{rel}^2\frac{\vec{v}_{rel}}{|\vec{v}_{rel}|} \tag{1}$$

where

$$\vec{v}_{rel} = \frac{d\vec{r}}{dt} - \vec{\omega}_{\oplus} \times \vec{r} \tag{2}$$

is the velocity vector relative to the rotating atmosphere; C_D is the coefficient of drag; A is the exposed cross-sectional area; m is the object's mass; $\vec{\omega}_{\oplus}$ is the mean motion of the Earth's rotation; and $\vec{r}$ is the Earth Centered Inertial object position vector [14]. The drag coefficient, mass, and area of the object are typically combined to form the the ballistic coefficient ($\beta = \frac{C_D A}{m}$).

1.2 Prior Work

The High Accuracy Satellite Drag Model (HASDM) project is an example of an empirical approach. This effort estimates a time-series of thirteen spherical harmonic global density and temperature correction coefficients in a batch fit by using observations of 75-80 carefully selected calibration satellites (payloads and debris objects) in a batch fit [1, 2, 10]. Intensive sensor tasking is made available for this effort, which allows for the collection of approximately 500 observations per day per calibration satellite. HASDM decouples the ballistic coefficient and the density parameter by first solving for the long-term averaged ballistic coefficient of each satellite, averaging almost 3200 previously estimated values for each calibration satellite.

The HASDM empirical model does not allow for the spatial and temporal resolution necessary to capture the dynamical behavior of density. As described above, this method estimates coefficients of density that are applied to a pre-defined model, not density directly. Furthermore, by combining information from objects in different regimes, or at different altitudes, a single batch fit limits the spatial resolution of density corrections that can be achieved.

More recently, density modeling and forecasting methods have been developed that take advantage of physics-based models. Matsuo [4] showed that ionospheric electron density data can be used to estimate driver parameters of the physics-based Thermosphere-Ionosphere-Electrodynamics General Circulation Model (TIE-GCM) [9] for the purpose of extending thermospheric mass density predictions. Mehta and Linares [5] developed an approach that aims to combine the strength of a physics based model in its predictive capability, with the speed of an empirical model. Their approach is demonstrated using an empirical model, MSIS, as the underlying upper atmosphere model with the intention that a physics-based model will replace MSIS in the future. A physics-based approach that estimates atmospheric drivers, such as F10.7 and Kp indices, as inputs to TIE-GCM is described by Sutton [12]. This effort estimates drivers through an iterative process that involves data assimilation of neutral density data from the Challenging Mini-Satellite Payload (CHAMP).

Our tool is named SoleiTool to emphasize its focus on the sun-driven nature of the near-Earth space environment. It takes advantage of a physics-based model, while leveraging routinely observed debris object data to estimate TIE-GCM forcing parameters, specifically Kp and F10.7 indices. The estimated Kp and F10.7 indices are then input to TIE-GCM to obtain a time-series of density, and can also be used in real-time or for atmospheric density predictions.

Our density estimation method is introduced in Section 2. Section 3 describes the scenario, including the simulated debris tracking data (debris objects, measurements, etc.) and filter initializations. The performance of SoleiTool when applied to this system is analyzed in Section 4. We conclude with a summary of findings and plans for future work.

2. METHOD

As shown in Fig. 1, SoleiTool comprises of two filters. The first filter utilizes debris object tracking data, in the form of measurements collected from ground sensors, to estimate acceleration due to atmospheric drag (a_{drag}), as well as the position and velocity (orbit determination state) of the debris objects. The total estimated state contains six orbit determination elements and one a_{drag} element per debris object. Debris object data are assimilated and the resulting estimated accelerations, as well as time, position, and velocity, are passed to the second filter. The filter type, measurements, and estimated states of both filters are summarized in Table 1.

Copyright © 2019 Advanced Maui Optical and Space Surveillance Technologies Conference (AMOS) – www.amostech.com

Table 1: UKF and PF Summary

Filter Type	**Measurements**	**Estimated State**
1. UKF	Debris Object az, el, range	Debris Object position, velocity, and a_{drag}
2. PF	a_{drag}	Kp, F10.7

The second filter, a Particle Filter (PF), processes accumulated estimates to produce Kp and F10.7 forcing parameters of a physics-based space environment model, TIE-GCM. Ensemble filters have typically been employed in high-dimensional non-linear geophysical applications, such as weather forecasting of atmosphere and ocean systems. However, in the framework proposed here, a PF provides a viable option for the second stage filter. Because our approach effectively reduces the state dimension, n, to only 2 forcing parameters, it becomes feasible to implement the necessary particle space of 10^n particles [7]. It is noted that our SoleiTool aims to estimate a time-series of Kp and F10.7 forcing parameters to TIE-GCM that will produce a density field that captures the true underlying density field; not necessarily to estimate the actual 3-hour global index of geomagnetic activity (Kp) and solar flux at a wavelength of 10.7 cm (F10.7) [13, 6].

TIE-GCM is used to generate a cloud of forecast density particles in the PF. The density particles, combined with the debris object ballistic coefficient and velocity, form predicted a_{drag} measurements. The PF applies corrections in the form of weight adjustments to the cloud of Kp and F10.7 particles based on the difference between these a_{drag} predictions and the first filter's a_{drag} estimates.

For the purpose of this study, the altitude of the debris objects are limited to 400 km altitude for simplification. In fact, the resulting estimated forcing parameters to TIE-GCM can be used to model density values for objects in LEO up to 700 km during solar max.

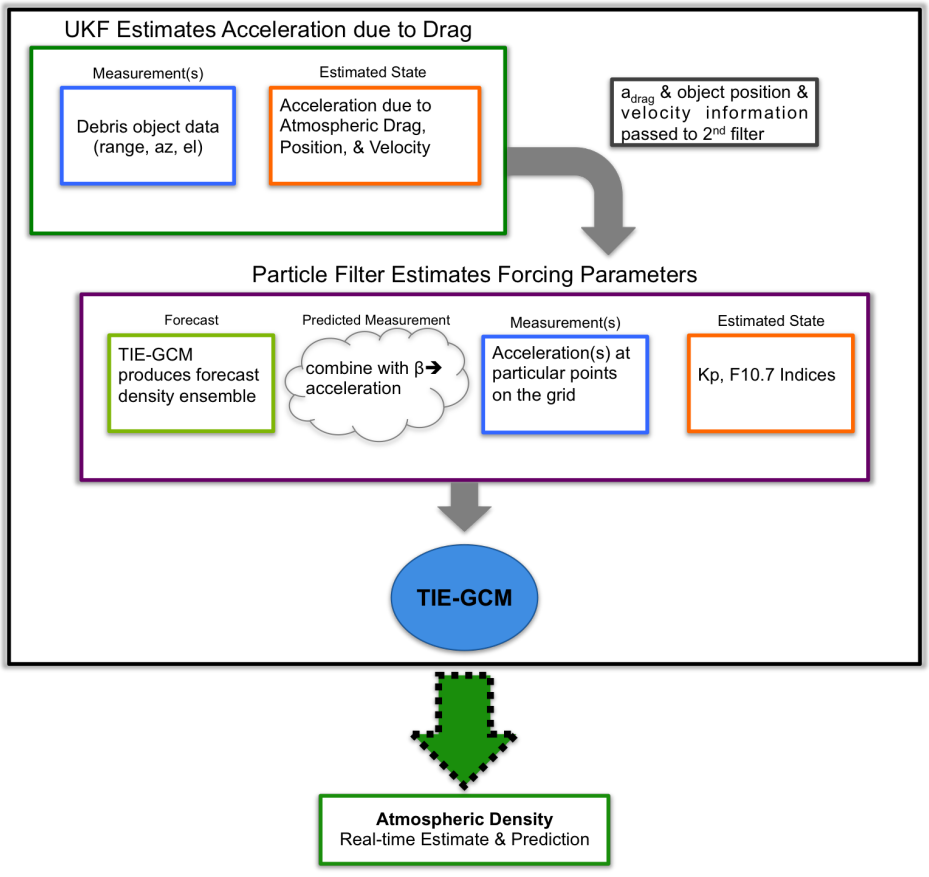

Fig. 1: SoleiTool Flow

Copyright © 2019 Advanced Maui Optical and Space Surveillance Technologies Conference (AMOS) – www.amostech.com

Our current approach assumes that the ballistic coefficients of debris objects are known to a reasonable accuracy. This assumption is based on the idea of initializing the ballistic coefficients with information from the HASDM, which is regularly used in operations for updated density estimates. To accomplish this, density information from HASDM, when available, will be combined with debris object measurements to infer debris object ballistic coefficients.

2.1 TIE-GCM

TIE-GCM is an open source general circulation model developed by the National Center for Atmospheric Research (NCAR) [8]. It is a three-dimensional, nonlinear representation of the coupled thermosphere and ionosphere system [11]. By adjusting model input parameters of the F10.7 index and Kp indices, TIE-GCM can simulate global thermospheric mass density changes under different solar extreme ultraviolet radiation and geomagnetic activity levels. For the purpose of this work, the model output time step is set to 1 hour and a default horizontal resolution of 5 degrees latitude and 5 degrees longitude is used with a vertical pressure level size of a half-scale height, extending from about 97 to 500 or 700 km (depending on solar cycles) [3]. Vertical interpolation is done during post-processing of the model output to obtain atmospheric density at 400 km altitude using the geopotential height. Interpolation is also executed in horizontal space and time to allow for a finer resolution of latitude, longitude, and time. In this work, Kp and F10.7 indices are estimated via assimilation of debris objects data in the PF.

3. SCENARIO

To develop the SoleiTool, we implemented a flexible simulation framework. Simulation details, such as debris objects, density field through which objects are propagated, and synthetic measurements are provided in Section 3.1. Initializations applied in both filters are described in Section 3.2.

3.1 Simulation Details

Fifteen debris objects are simulated for 650 minutes (roughly 11 hours). The objects are put in circular orbits with an initial altitude of 400 km. The remaining orbital parameters are distributed over the range provided in Table 2.

Table 2: Debris Object Orbital Elements

	Inclination	Initial True Anomaly	Right Ascension of Ascending Node
Minimum Value	10°	0°	0°
Maximum Value	45°	359 °	46°

The objects are propagated using two-body Keplerian dynamics plus atmospheric drag perturbations,

$$\ddot{\vec{r}} = \frac{\mu}{\vec{r}^3}\vec{r} - \frac{1}{2}\rho\frac{C_D A}{m}v_{rel}^2\frac{\vec{v}_{rel}}{|\vec{v}_{rel}|} \tag{3}$$

where $\vec{v}_{rel}$ is defined in Eq. 2. The underlying density field through which the objects travel is generated via TIE-GCM. Calm conditions (low geomagnetic activity) are simulated using Kp and F10.7 index values of 3.166 and 127, respectively. The resulting density is shown in Fig. 2.

Copyright © 2019 Advanced Maui Optical and Space Surveillance Technologies Conference (AMOS) – www.amostech.com

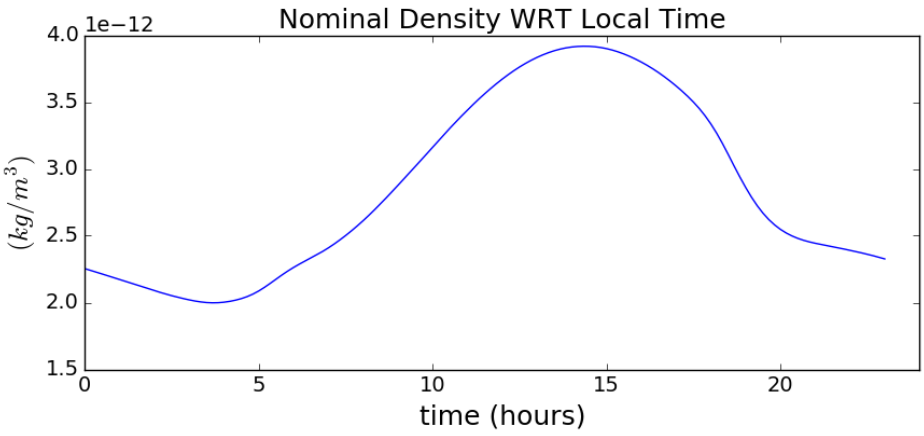

Fig. 2: Nominal Density Field Generated by TIE-GCM for a Particular Location on the Equator

Each object is simulated with an area to mass ratio (AMR) of 0.0955 m^2/kg. Nominally, the filter also assumes this correct AMR value of each object. Azimuth (az), elevation (el), and range (R) measurements of the objects are generated from the ground stations located in Canberra, Madrid, Diego Garcia, California, and Maui (red stars in Fig. 3). Measurements are collected at a 3-minute cadence when objects are visible from a ground station. An azimuth and elevation sensor error standard deviation of 0.25 arc-seconds and range sensor error standard deviation of 0.25 meters is applied to the measurements. The ground track of one orbital period for each debris object is shown in Fig. 3.

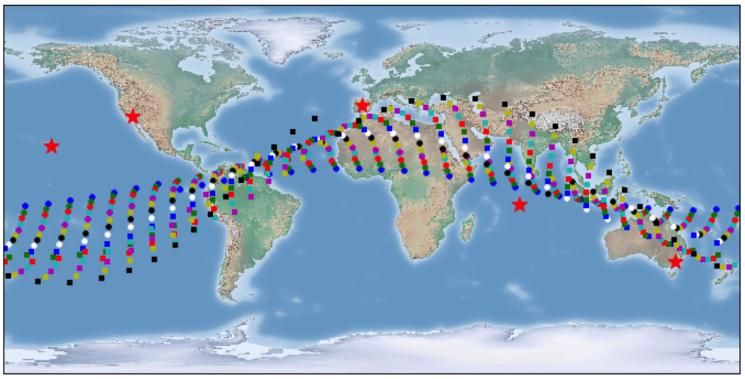

Fig. 3: One Orbital Period Groundtrack of Debris Objects

3.2 Initialization

In the UKF, the orbit determination (OD) state is defined as the position and velocity of each object:

$$\vec{X} = [\vec{r}, \vec{v}]^T \tag{4}$$

A perturbation is applied to the true initial a_{drag} and OD state so that the *a priori* state in the filter is not exactly equal to the true initial state,

$$\vec{X}_0' = \vec{X}_0 + \vec{p} \tag{5}$$

where

$$\vec{p}_{OD} = [100m, 100m, 100m, 0.1m/s, 0.1m/s, 0.1m/s]^T \tag{6}$$

and

$$\vec{p}_{a_{drag}} = \left[5e-5cm/s^2\right]^T \tag{7}$$

Copyright © 2019 Advanced Maui Optical and Space Surveillance Technologies Conference (AMOS) – www.amostech.com

It is noted that the true a_{drag} is on the order of 0.001 cm/s^2. Sigma points are generated using the perturbed initial state ($\vec{X}_0'$) and its *a priori* statistical information (P_0):

$$P_{0\ OD} = diag\left(\left[(150m)^2,(150m)^2,(150m)^2,(0.15m/s)^2,(0.15m/s)^2,(0.15m/s)^2\right]\right) \tag{8}$$

and

$$P_{0\ a_{drag}} = diag\left(\left[12e-5cm/s^2\right]\right) \tag{9}$$

In the second filter, the PF, a similar approach is taken. A perturbation is applied in the PF to the true initial Kp and F10.7 index state (Eq. 5), where

$$\vec{p} = [0.5, 15]^T \tag{10}$$

An initial cloud of Kp and F10.7 particles (χ_0) is generated using the perturbed initial state ($\vec{X}_0'$) and its *a priori* statistical information (P_0):

$$\chi_0^{(i)} = \vec{X}_0' + \eta^{(i)} \tag{11}$$

where,

$$\eta^{(i)} \sim \mathcal{N}(0, P_0) \tag{12}$$

and

$$P_0 = diag\left(\left[(0.85)^2,(30)^2\right]\right) \tag{13}$$

Fig. 4 is the density generated via TIE-GCM using the initial 100 Kp and F10.7 particles. It shows the density for a single location on the equator as a function of local time. As expected, the maximum density occurs just after local noon. The maximum density achieved, around 9e-12 kg/m^3, is about 5e-12 kg/m^3 larger than the maximum density for nominal conditions (Fig. 2). This range of densities from the initial Kp and F10.7 particles is necessary in order to capture the possible state space.

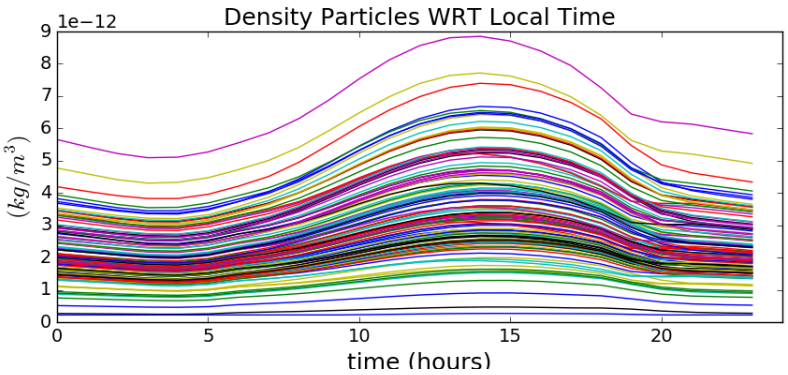

Fig. 4: TIE-GCM Density as Generated from 100 Particles

4. RESULTS

The results of the UKF and PF are presented and analyzed separately in Sections 4.1 and 4.2.

4.1 First Filter: UKF

The UKF ingests debris object tracking data to estimate a_{drag}, position, and velocity of the debris objects. Fig. 5 shows the true and estimated along-track acceleration due to drag for one debris object at the times that measurements are available. The true a_{drag} is cyclical because the debris object experiences areas of low (near local midnight) and high (near local noon) atmospheric density throughout one orbital period of 90 minutes. The estimated a_{drag} lags the true a_{drag} during the first 90 minutes. After about one orbital period, the UKF is able to better track the changing a_{drag} and follow its cyclic nature. It is apparent that the filter has more difficulty tracking the time-varying a_{drag} when the

Copyright © 2019 Advanced Maui Optical and Space Surveillance Technologies Conference (AMOS) – www.amostech.com

measurements are more sparse. This demonstrates the advantage of utilizing multiple debris objects. Some objects will provide more accurate a_{drag} estimates at times that other objects a_{drag} estimates have larger errors. When combined, they provide enough information to estimate TIE-GCM forcing parameters in the second filter, the PF.

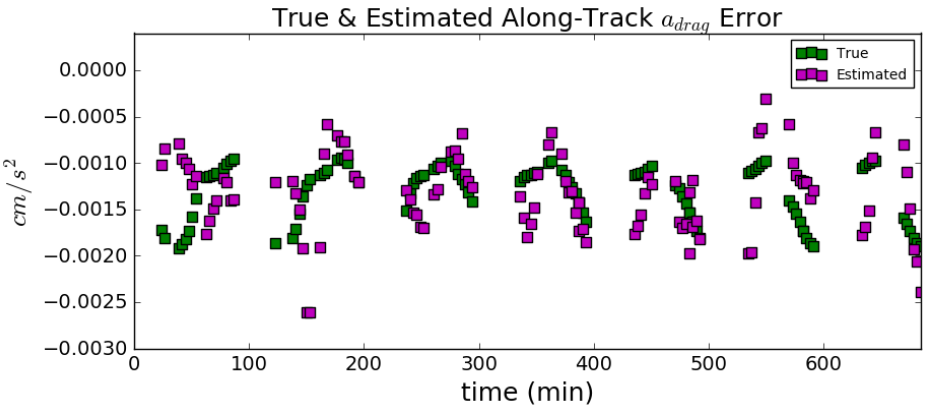

Fig. 5: Estimated v. True Along-track a_{drag} for One Object

Fig. 6 is the estimated along-track a_{drag} for all 15 objects in the scenario. The first 90 minutes are not shown because only measurements beginning after filter convergence are ingested by the PF. These UKF estimated a_{drag} and corresponding variance time-series are then input as measurements and measurement uncertainty in the PF.

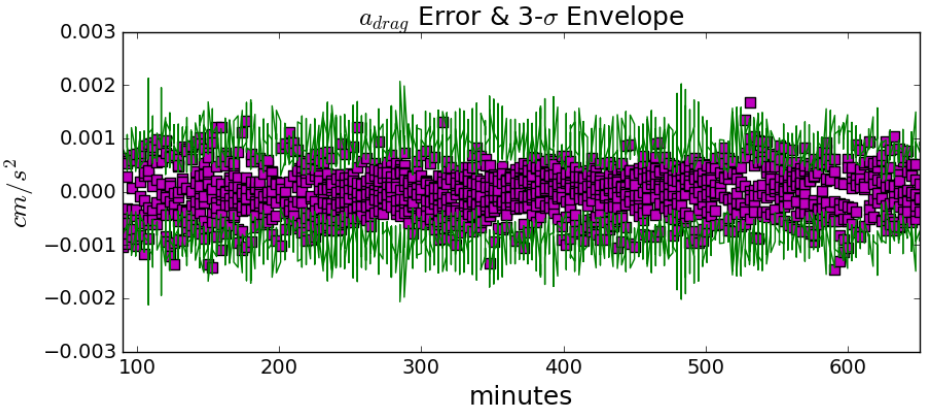

Fig. 6: Multi-Object Along-track Acceleration Error and 3-σ Envelope

4.2 Second Filter: PF

The PF uses the accumulated a_{drag} estimates from the UKF to produce Kp and F10.7 forcing parameters of TIE-GCM. Figs. 7 and 8 show the time evolution of the estimated Kp and F10.7 particles. The initial distribution collapses after the first few measurements. We inject a continual spreading of particles after the initial collapse by adding process noise to the particles in the time update. The Kp and F10.7 particle distribution is offset from the truth initially due to the perturbation applied to the *a priori* (described in Section 3.2). Both particle distributions trend slightly away from the true indices (3.166 Kp and 127 F10.7) within the first 100 minutes of measurements; the estimated F10.7 trends low while the estimated Kp trends high. This may be indicative that the two inputs (F10.7 and Kp) are strongly correlated with respect to the synthetic data used. In other words, within TIEGCM, the two effects are compensating; the effect of a low F10.7 on density can be somewhat canceled by a high Kp. The time-series of estimated Kp and F10.7 indices are used as input to TIE-GCM to generate what we'll call the *estimated* density. Because the goal of our tool is to estimate forcing parameters that produce the true underlying density in TIE-GCM, the tool performance is

Copyright © 2019 Advanced Maui Optical and Space Surveillance Technologies Conference (AMOS) – www.amostech.com

evaluated by comparing the true and estimated density.

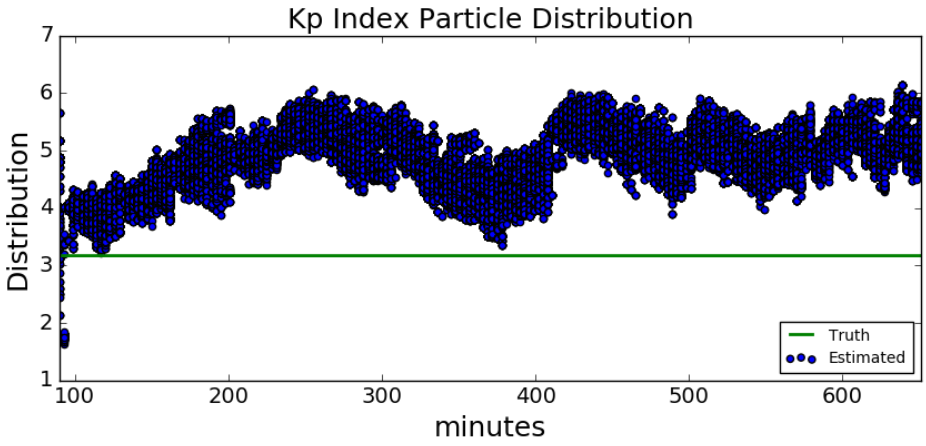

Fig. 7: Time Evolution of Kp Index Particles

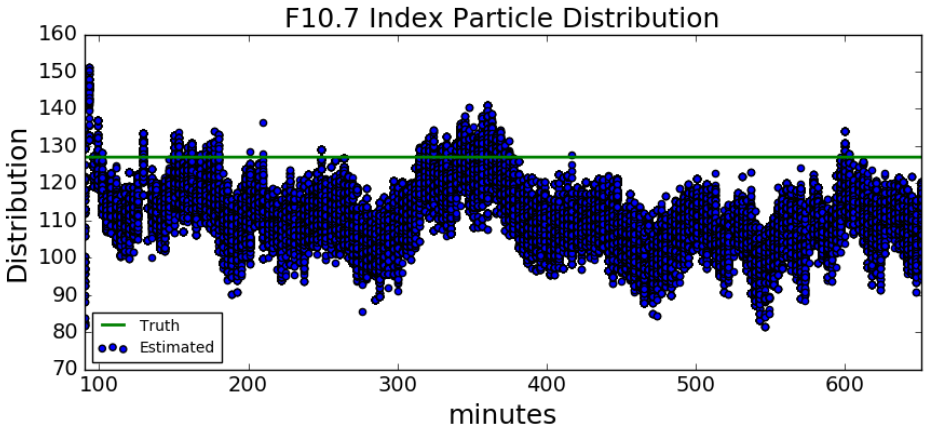

Fig. 8: Time Evolution of F10.7 Index Particles

The estimated and true density along one object's trajectory are shown in Fig. 9. The magenta markers represent measurement times of this debris object. We see that the estimated density has relatively large error compared to the true density in the beginning of the simulation, but then starts to follow the same smooth cyclic nature as the true density for the remainder of the simulation. Fig. 10 shows the estimated density error and its 3-σ bounds for this object.

Copyright © 2019 Advanced Maui Optical and Space Surveillance Technologies Conference (AMOS) – www.amostech.com

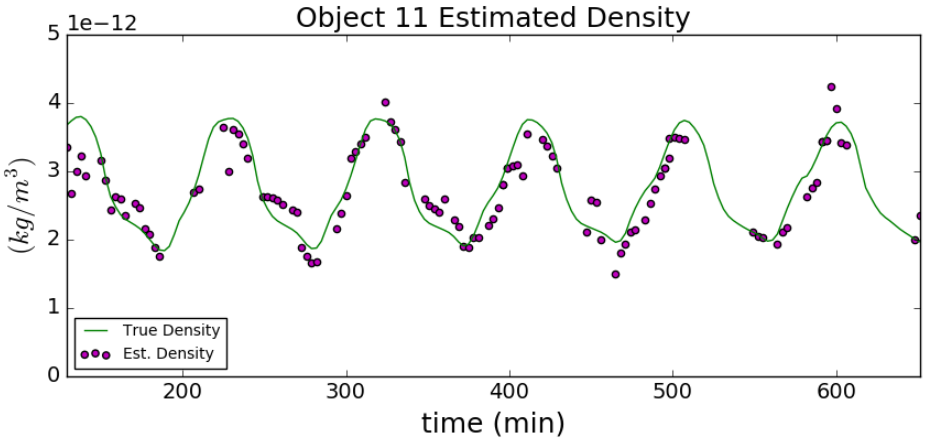

Fig. 9: Density Generated from Estimated TIE-GCM Kp and F10.7 Indices v. True Density for a Single Object

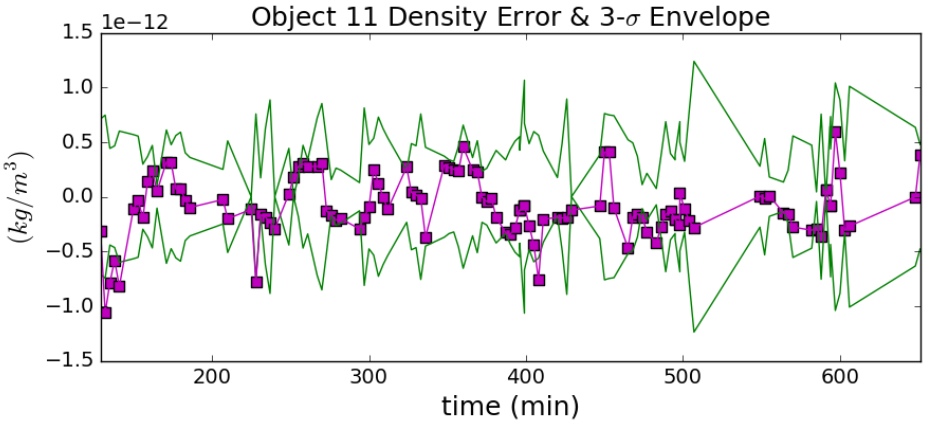

Fig. 10: Density Error and 3-σ Envelope for a Single Object

All the object results are combined to show the overall PF performance in Fig. 11. This plot shows the time-series of the density error and 3-σ envelope at all measurement times (regardless of object). The 3-σ bounds are computed using the spread of density values produced in TIE-GCM via the cloud of state particles (Kp and F10.7) at each measurement time.

Copyright © 2019 Advanced Maui Optical and Space Surveillance Technologies Conference (AMOS) – www.amostech.com

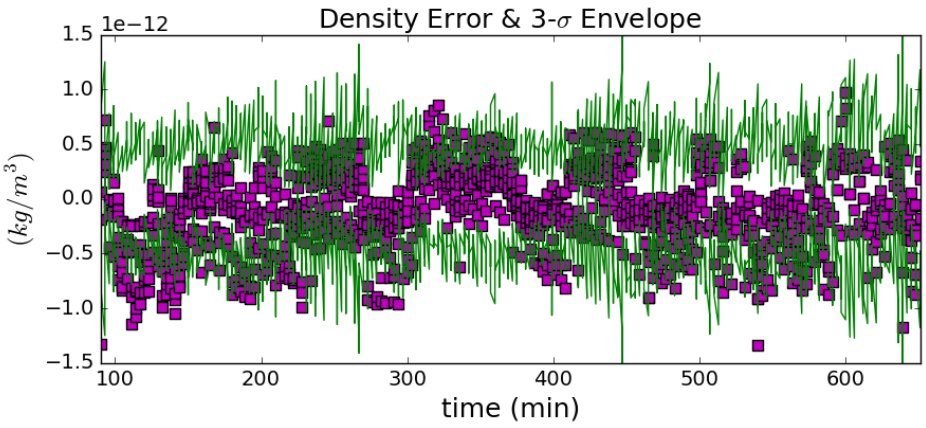

Fig. 11: Density Error and 3-σ Envelope

5. CONCLUSION AND FUTURE WORK

Our work shows the potential for operationally collected debris object tracking data to be utilized to derive atmospheric density in LEO. The proposed two-filter process ingests debris object tracking data and first estimates a time-series of acceleration due to drag, before passing these estimates to the second filter to be used as measurements. The second filter, the PF, estimates Kp and F10.7 indices. These forcing parameters are input to TIE-GCM to produce an informed estimate of atmospheric density. SoleiTool also provides a predictive capability; forcing parameters can be utilized in TIE-GCM to forecast the near Earth space environment.

Although simulated tracking data from only 15 debris objects were used for this paper, we plan to demonstrate the performance of SoleiTool with hundreds to thousands of debris objects. By adding substantially more debris objects with greater variation in orbital elements, we plan to get an improved global picture of densities. A geomagnetic storm scenario will also be investigated in order to determine how well the filter is able to track time-varying Kp and F10.7 indices that increase to values as high as 9 and 273, respectively, for an extreme geomagnetic storm [13].

In order to make a more realistic scenario, various object AMRs will be simulated and imperfect knowledge of object AMRs assumed in the filter. Spinning objects will also be incorporated so that the object area considered in the equation for acceleration due to drag is not constant. Currently, only Kp and F10.7 indices are estimated in the PF; however, there are several other available input parameters to TIE-GCM. We plan to investigate estimation of additional TIE-GCM forcing parameters. Closed-loop feedback from the PF to UKF will also be considered in order to allow for an improved initialization of along-track a_{drag}.

6. ACKNOWLEDGMENTS

Support for S. Mutschler has been provided by the National Defense Science and Engineering Graduate (NDSEG) Fellowship. We thank Chih-Ting Hsu, a postdoctoral fellow at University of Colorado Boulder, for her assistance with TIE-GCM.

Copyright © 2019 Advanced Maui Optical and Space Surveillance Technologies Conference (AMOS) – www.amostech.com

7. REFERENCES

1. Bowman, B., Storz, M.F., 2002. Time Series Analysis of HASDM Thermospheric Temperature and Density Corrections. In: AIAA/AAS Astrodynamics Specialist Conference.

2. Bowman, B., Storz, M.F., 2003. High accuracy satellite drag model (HASDM) review. *Advances in the Astronautical Sciences*. 116. 1943-1952.

3. Matsuo, T., Lee, I.-T., Anderson, J.L., 2013. Thermospheric mass density specification using an ensemble Kalman filter. *Journal of Geophysical Research*. Space Physics. 118. 1339-1350. 10.1002/jgra.50162.

4. Matsuo, T., 2014. Upper atmosphere data assimilation with an ensemble Kalman filter. In: Qian, L., Burns, A.G., Emery, B.A., Foster, B., Lu, G., Maute, A., Richmond, A., Roble, R.G., Solomon, S., Wang, W., 2014. *Modeling the Ionosphere-Thermosphere System*. 10.1002/9781118704417.ch7.

5. Mehta, P., Linares, R., 2017. A methodology for reduced order modeling and calibration of the upper atmosphere. *Space Weather*. 15 (10),1270-1287.

6. NOAA Space Weather Scales, 2011. Space Weather Prediction Center www.swpc.noaa.gov/noaa-scales-explanation (accessed 10.1.18).

7. Psiaki, Mark. 2013. The blind tricyclist problem and a comparative study of nonlinear filters: A challenging benchmark for evaluating nonlinear estimation methods. *Control Systems, IEEE*. 33. 40-54. 10.1109/MCS.2013.2249422.

8. Qian, L., et al. (2014), The NCAR TIE-GCM: A community model of the coupled thermosphere/ionosphere system. In: *Modeling the Ionosphere-Thermosphere*. Geophysical Monograph Series, vol. 201, edited by J. D. Huba, pages 73-83., AGU, Washington, D. C, doi: 10.1002/9781118704417.ch7.

9. Richmond, A.D., Ridley, E.C., Roble, R.G., 1992. A thermosphere/ionosphere general circulation model with coupled electrodynamics. *Geophysical Research Letters*. 19, 601?604, doi:10.1029/92GL0040.

10. Storz, M.F., Bowman, B.R., Branson, J.I., Casali, S.J., Tobiska, W.K., 2005. High Accuracy Satellite Drag Model (HASDM). *Advances in Space Research*, 36 (12), 2497-2505.

11. Sutton, E., Cable, S., Lin, C., Qian, L., Weimer, D.R., 2012. Thermospheric basis functions for improved dynamic calibration of semi-empirical models. *Space Weather*. 10. 10.1029/2012SW000827.

12. Sutton, E., 2018. A New Method of Physics-Based Data Assimilation for the Quiet and Disturbed Thermosphere. *Space Weather*. 16 (6), 736-753.

13. Thompson, R., Space Weather Indices, Australian Government Bureau of Meteorology www.sws.bom.gov.au/Educational/1/2/4 (accessed 10.1.18)

14. Vallado, D.A., 2013. *Fundamentals of Astrodynamics and Applications*. Space Technology Library.

Copyright © 2019 Advanced Maui Optical and Space Surveillance Technologies Conference (AMOS) – www.amostech.com